Terahertz radiation from shocked materials

Distinct physical mechanisms for the generation of temporally coherent, narrow bandwidth optical radiation are few and rare in nature. Such sources, including lasers, have widespread applications ranging from spectroscopy to interferometry. We review the recent theoretical prediction of a new type of temporally coherent optical radiation source in the 1-100 THz frequency range that can be realized when crystalline polarizable materials like NaCl are subject to a compressive shock wave.

Evan J. Reed[1,2,*], Michael R. Armstrong[1], Kiyong Kim[3], Marin Soljačić[2], Richard Gee[1], James H. Glownia[3], and John D. Joannopoulos[2]

[1]Lawrence Livermore National Laboratory, Livermore, CA 94551, USA

[2]Center for Materials Science and Engineering and Research Laboratory of Electronics, Massachusetts Institute of Technology, Cambridge, MA 02139, USA

[3]Center for Integrated Nanotechnologies, Los Alamos National Laboratory, Los Alamos, NM, USA

**E-mail: reed23@llnl.gov*

While technological advances in existing types of optical sources are likely to define the near future, new and as yet unrealized mechanisms of light generation may play a significant role further into the future. This may be particularly true in the terahertz frequency regime where sources and detectors are an active field of development[1]. Loosely defined from 300 GHz to 20 THz, this regime falls between the infrared and microwave regions of the electromagnetic spectrum where optical techniques are pushed to their lower frequency limits and electronics-based techniques are pushed to their upper frequency limits. Improving the capabilities of terahertz technology is enabling potential applications including nondestructive material characterization, remote sensing and communications, new methods of medical and biological imaging, and security screening devices[2,3]. A wide array of terahertz sources and detectors are under development and recent work includes the development of active terahertz materials[4,5]. The latest developments are summarized elsewhere[5-7].

We review new mechanisms of terahertz radiation generation that are based on the formation of shock waves in materials. A new type of weak but narrow-band, temporally coherent electromagnetic radiation source in the 1-100 THz frequency range can be predicted when crystalline polarizable materials are subject to a shock wave excitation[8-10]. Rather than resulting from lasing in a cavity, the radiation is generated by an oscillating material polarization resulting from the synchronized nonresonant motion of large numbers of atoms induced in the nonequilibrium region at the front of a planar shock wave propagating through the crystalline lattice. The mechanism responsible for this type of emission is fundamentally distinct from existing sources of many-cycle, temporally coherent optical radiation in this frequency regime. These include 'traditional' lasers based on stimulated emission, free-electron lasers[11], and phonon-related mechanisms[12]. The coherence of the emitted radiation comes from the spatial coherence of the crystalline lattice and the constant propagation speed of the shock wave.

ISSN:1369 7021 © Elsevier Ltd 2007

Commonly employed mechanisms for generating terahertz frequency light include nonlinear optical processes with subpicosecond pulse lasers[5], terahertz laser devices (e.g.[13]), and free-electron lasers (e.g.[14]). Here we describe a different mechanism of terahertz frequency generation that uses the nonlinear acoustic response of a material. A strain wave or sound wave of an amplitude sufficient to generate a nonlinear acoustic response will tend to develop high-frequency components as it propagates (e.g.[15]). Fig. 1 shows a molecular dynamics simulation of a strain wave generated in crystalline GaN. The initial rise time of the strain wave is 3 ps but the rise time decreases to <1 ps as it propagates. In principle, a strain wave with any rise time input into a material can be made to steepen up to the picosecond timescale given sufficient propagation distance and strain amplitude. Therefore, high-frequency strain components can be generated from much lower, more readily generated frequencies. The steepening process in crystals can occur until the spectral components of the rise time of the wave are comparable to the highest acoustic frequency phonons in the material, typically in the range of 1-10 THz.

Historically, shock waves have been generated in the laboratory for the purpose of studying the high pressure and temperature properties of materials. Shock waves are generated using a variety of techniques including high-velocity projectiles fired from cannons and pulsed lasers. They are often single-shot, destructive experiments in which the shocked material is irreversibly altered, but the experiments can leave the material unaltered if the shock amplitude and duration are sufficiently small, typically with strains ~1%. While a practical device that uses a cannon may be rather inconvenient, tabletop lasers with high-repetition rates and short pulses (<100 fs) of millijoule energies are sufficient to generate shock waves in materials (e.g.[16,17]).

In addition to the temporally coherent mechanism discussed here, it is likely that ultrafast timescale phenomena in shocked polarizable materials can lead to terahertz frequency radiation emission through a wide variety of mechanisms, including fast phase transformations like melting of a pyroelectric material. At much lower (megahertz) frequencies, large-amplitude radio-frequency voltage spikes have been observed in shock-depolarized ferroelectrics[18]. Similar phenomena may occur at higher frequencies, but terahertz radiation is not typically (if ever) probed in shock wave experiments.

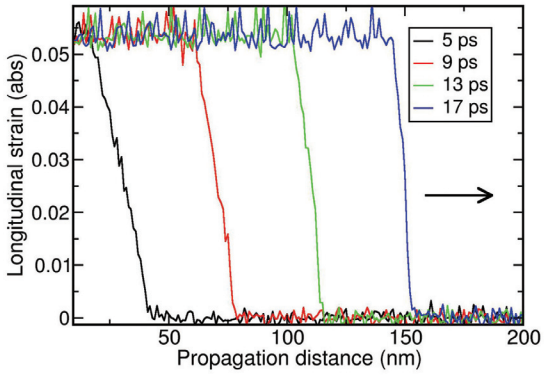

Fig. 1 Molecular dynamics simulation of a shock wave front steepening with time. The initial rise time of the strain wave is 3 ps but the rise time decreases to less than 1 ps as it propagates because of nonlinear elastic material properties that result in higher frequency strain components. In principle, this process can be used to generate high-frequency terahertz signals from much lower frequencies.

We are currently engaged in experimental work to look for terahertz emission from shocked materials using ultrafast laser-based techniques for high-repetition rate shock wave generation. Our initial experiments show terahertz signals in the range of 1-10 V/cm can be observed emerging from a shocked material and related to processes within the shock wave. While this review is primarily of theoretical scope, our initial observations of terahertz radiation from a shocked material indicate that reduction to practice may not be far into the future. We believe that initially such sources are most likely to be useful for ultrafast shock wave diagnostics.

Physical intuition for the origin of coherent radiation

It is well known that shock waves can induce static polarizations in a variety of materials[19,20]. For some distance behind the planar shock front, materials are typically characterized by a state of increasing uniaxial stress, i.e. the spatial gradient in the shock propagation direction component of the stress is nonzero. Such a spatial stress gradient breaks any inversion symmetry of the material by establishing a unique direction in the shocked material. The broken symmetry can lead to a static electric polarization along the shock propagation direction in any material, including isotropic liquids like water[21].

Here we review a special case of shock-induced polarization that occurs only in crystalline materials when the shock front becomes very sharp, i.e. the shock front rise distance is a few lattice planes of the crystal or less. Fig. 2 depicts how a temporally periodic polarization can arise in a shocked polarizable crystal as a result of athermal motion of the atoms. As the shock propagates over each lattice plane (left to right), the symmetry of atoms in that lattice plane can be temporarily broken to yield a nonzero static polarization of the atoms at the shock front. In Fig. 2, the static polarization points perpendicular to the plane of the shock wave. The broken symmetry can result from the atoms being of different types with different masses or it can have other origins. A transient static polarization is produced each time the shock propagates through a lattice plane of the crystal. This process gives a temporally periodic polarization current that can potentially emit coherent radiation.

The frequencies of these polarization oscillations can be shown to be of the form:

$$\omega = 2\pi l v_s / a \quad (1)$$

where v_s is the shock speed, a is crystal lattice constant, and l is an integer. These frequencies are integral multiples of the inverse time required for the shock to traverse a lattice unit of the crystal. For

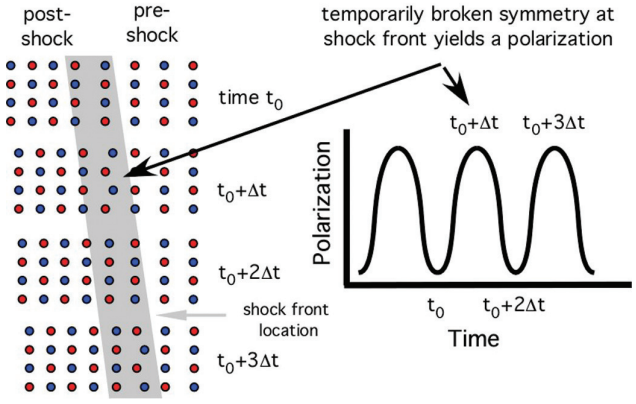

Fig. 2 Schematic showing how a temporally periodic polarization can arise in a shocked polarizable crystal. Red and blue atoms on the left represent positively and negatively charged atoms. Atom positions within the shocked crystal are shown at four instances in time on the left with a gray area highlighting the shock front region. As the shock propagates over each lattice plane (left to right), the symmetry of atoms in that lattice plane can be temporarily broken to yield a nonzero static polarization at the shock front. The static polarization disappears in the material behind the shock front. This process yields a temporally periodic polarization current that can potentially emit coherent radiation.

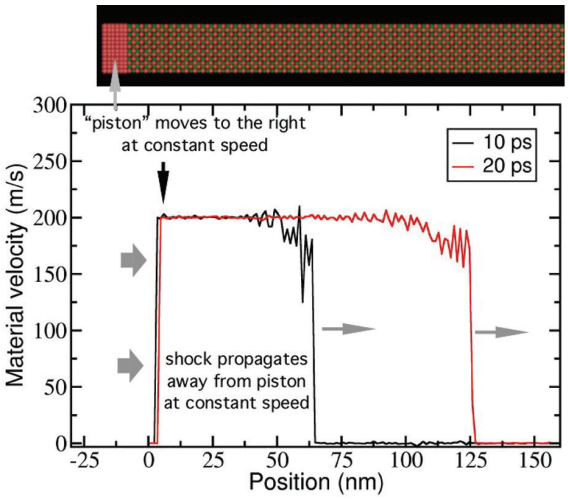

Fig. 3 Material speed as a function of position in a molecular dynamics simulation of a shock propagating in the [100] direction in NaCl. A 'piston' exists on the left side of the computational cell consisting of atoms with infinite mass fixed in the crystal structure (top). The piston is given a velocity of 200 ms^{-1} that drives a shock to the right. For clarity, the dimensions of the computational cell shown are reduced from those employed in the simulation.

typical ionic crystal lattice constants (0.1-1 nm) and typical shock speeds in these materials (1-10 kms^{-1}), the coherent oscillation frequencies lie in the range from 1-100 THz, i.e. the infrared and below into the terahertz frequency regime. The discrete nature of these frequencies indicates that a significant degree of temporal coherence can be achieved, if the shock speed and crystal lattice constants are fixed. Eq 1 describes frequencies that are not optical phonon frequencies of the crystal unless by coincidence.

Molecular dynamics simulations: coherent polarization currents

Eq 1 indicates that polarization oscillations at terahertz frequencies can be produced by a shock wave propagating through a polarizable crystal, but says nothing about the amplitude of the polarization oscillations. To assess the amplitude, we have explored the polarization currents generated by a shocked polarizable material numerically by performing molecular dynamics simulations of shock waves propagating through crystalline NaCl[10]. Shock wave molecular dynamics simulations solve the classical equations of motion for atoms subject to an empirically constructed interaction potential and incorporate thermal effects and deformation of the crystal lattice. Such simulations are commonly employed to study shock waves in a variety of materials (e.g.[22,23]). In these calculations, planar shock waves are generated within three-dimensional computational cells of perfectly crystalline rocksalt atoms (2-3 million atoms) by constraining the atoms at one edge of the long dimension of the computational cell to move into the cell like a planar piston (representing the mechanical driving force or object that generates the shock).

Fig. 3 shows the local material velocity as a function of position within the computational cell in the shock propagation direction for a typical shock simulation. The shock front is characterized by a rapid transition between material at rest and material moving with the piston speed (u_p = 200 ms^{-1} in this case). The shock front rise distance is about 1 nm, or about three to four lattice planes. The polarization currents generated in the computational cell can ultimately be related to the electromagnetic emission.

Fig. 4 shows the polarization current for simulations of shocks propagating in the [111] and [100] directions over ~30 ps duration that were initiated with piston velocities of 200 ms^{-1}. This relatively small piston velocity generates a shock that applies a uniaxial strain of 0.03-0.04 to the post-shock material and increases the material temperature <1 K. Such strains are readily achievable experimentally using gun-driven projectile impacts (e.g.[24]) and other approaches. Fig. 4 compares the shocked and unshocked Fourier transform of the shock propagation direction component of the total electric polarization current in the computational cell. Narrow peaks are observed in the shocked simulation that do not exist in the unshocked simulation.

The frequencies of the observed peaks agree well with eq 1, which predicts that polarization currents should occur in multiples of 5.4 THz in the [111] case since a = 9.78 Å for the [111] direction in NaCl and the shock speed observed in the simulation is v_s = 5300 ms^{-1}. The 16 THz and 32 THz peaks on the left of Fig. 4 correspond to three and six times the fundamental frequency of 5.4 THz (l = 3 and l = 6 in eq 1), in excellent agreement with theory (gray arrows). The 16 THz l = 3 peak can be attributed to structure within the unit cell of distance a = 3.26 Å (i.e. l = 1 if a = 3.26 Å in eq. 1), which is the distance

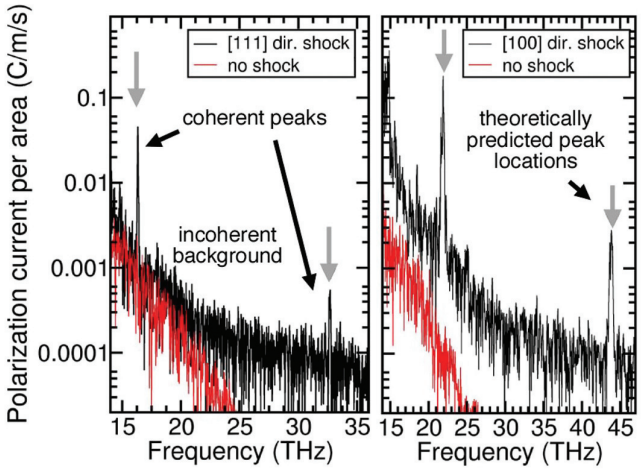

Fig. 4 Fourier transform of the electric polarization surface current component in the shock propagation direction for molecular dynamics simulations of a shock propagating through NaCl in the [111] direction (left) and [100] direction (right). Narrow bandwidth, coherent peaks exist in the shocked simulations (black) that do not exist in the unshocked simulations. Gray arrows are emission frequencies predicted by eq 1. Thermal noise gives rise to an incoherent background. (Reprinted with permission from[8]. © 2006 American Physical Society.)

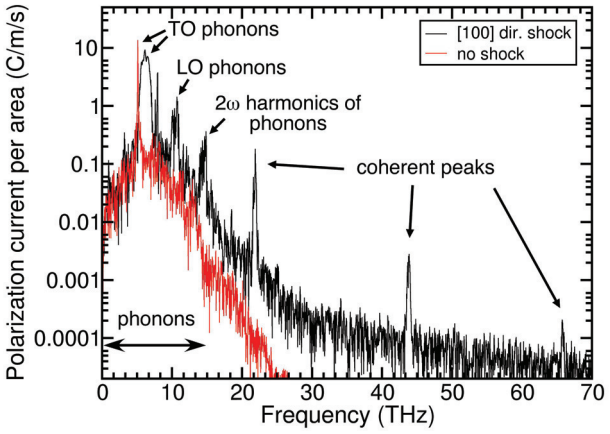

Fig. 5 Electric polarization surface current component in the shock propagation direction for molecular dynamics simulations of a shock propagating through NaCl in the [100] direction. The shocked simulation (black) contains a number of excitations that are not present in the unshocked simulation (red). These include the longitudinal-optical (LO) phonons, harmonics of lower frequency phonons, and the higher frequency narrowband excitations discussed in this work. Transverse-optical (TO) phonons are also visible in both the shocked and unshocked simulations.

between atomic lattice planes of like charge in the [111] direction (the NaCl crystal consists of alternating planes of positively and negatively charged atoms in the [111] direction). Lattice planes are compressed as the shock propagates through the crystal, generating an alternating polarization current with a frequency associated with the rate at which the shock propagates through the lattice planes. Peaks corresponding to other *l* values are suppressed because of the symmetry properties of the unit cell: the planar shock wave induces identical polarizations in different lattice planes within the unit cell.

If the shock speed is constant, the generated frequencies are constant and the coherence time of the emitted radiation is expected to be proportional to the time duration of the propagation of the shock wave. From the peak widths, the coherence time of the polarization current is determined to be about 17 ps and 10 ps for the 16 THz [111] peak and 22 THz [100] peak, respectively (200-300 cycles). For radiation emitted into vacuum, these coherence times correspond to coherence lengths of 5 mm and 3 mm, respectively. The coherence times are nearly Fourier-transform-limited (simulation durations are around 30 ps), suggesting that longer coherence lengths might be possible by increasing the shock propagation time. It is expected that the magnitude of fluctuations in the shock propagation speed will likely determine the coherence time of the polarization currents.

Fig. 5 shows the full spectrum of the [100] direction shock in Fig. 4. In addition to the narrowband peaks at multiples of 22 THz, there are phonon-related peaks that arise at lower frequencies. The coherence time of an impulsively excited optical phonon is given by a decay or dephasing time, while the coherence time of the shock mechanism is independent of such dephasing mechanisms.

Fig. 6 shows Fourier transforms of the electric polarization surface current component in the shock propagation direction for the simulation in Fig. 5. On the left is a plot of frequency as a function of time (the Fourier transform window length for each time on this plot is 5 ps). This plot shows that the 22 THz signal occurs for the duration of the shock propagation. On the right side of Fig. 6 is a plot of frequency as a function of position in the computational cell in the shock propagation direction. During the time window over which this Fourier transform is taken (from 5 ps to 15 ps), the shock front propagates between the white dotted lines. The polarization current at 22 THz occurs in the region where the shock front is located rather than behind it or in front of it, consistent with the schematic in Fig. 2. This indicates that the excitation is nonresonant and leaves no excitation at 22 THz in the wake of the shock. Such behavior is expected since the highest (linear) phonon frequencies are far lower, around 11 THz.

While the initial material temperature in these simulations is 4 K, we find that the signal can be observed above the thermal background at higher temperatures, including room temperature under some conditions. Increasing the shock amplitude (pressure) can increase the polarization current magnitudes by a factor of ten or potentially more.

Radiation emission characteristics

The molecular dynamics simulations yield polarization currents but they do not explicitly solve Maxwell's equations for the electric and magnetic fields that radiate away from the shock wave. However, since the wavelength of radiation emitted at frequencies considered here (>10 μm) is much longer than the dimensions of the computational cell, the total polarization current generated in the computational

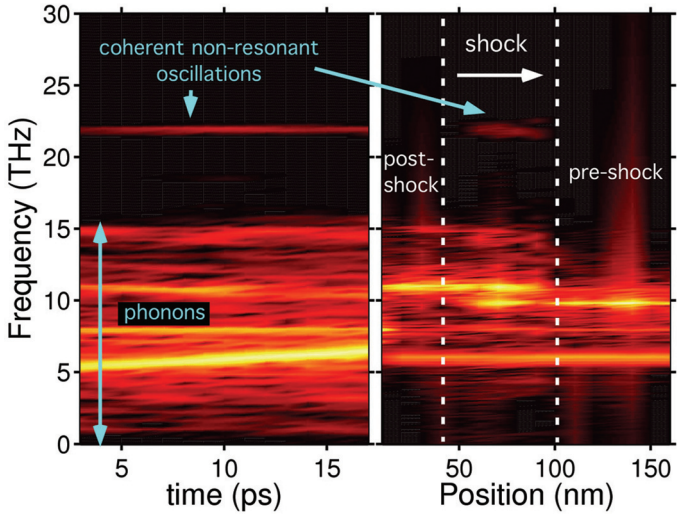

Fig. 6 Electric polarization surface current component in the shock propagation direction for molecular dynamics simulations of a shock propagating through NaCl in the [100] direction. (Left) The 22 THz signal (nonresonant) polarization current occurs for the duration of the shock propagation with roughly constant amplitude. (Right) Plot of frequency as a function of position in the computational cell in the shock propagation direction. During the time over which this Fourier transform is taken, the shock front propagates between the white dotted lines. The 22 THz current occurs in the region where the shock front is located rather than behind it or in front of it.

cell is closely related to the generated electromagnetic radiation for frequencies above the phonon frequencies (above ~10 THz in this NaCl model) where the material has good transmission properties. At lower frequencies, the relationship is complicated by absorption and polariton gaps. We have focused on determination of the electromagnetic emission for frequencies above the phonon frequencies where the material is transparent.

The shock waves in the molecular dynamics simulations are planar, but deviations of the shock front from perfect planarity are inevitable experimentally and can have a significant effect on emission characteristics. Fig. 7 shows how variations of the flatness of the shock front on the length scale of $2\pi v_s/\omega$ (on the order of angstroms) can yield spatial variations in the phase of the oscillating polarization current. Through a phase-matching condition, the phase of the oscillating polarization current can affect the distribution and intensity of the emitted radiation. The presence of crystal

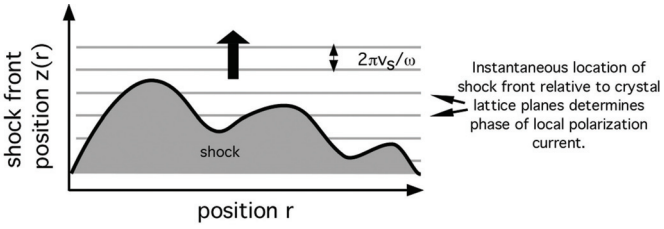

Fig. 7 Schematic of variations in the shock front position, z(r), superimposed on periodic units of the crystal (e.g. lattice planes). The phase of the polarization current depends very sensitively on the flatness of the shock front on the length scale of $2\pi v_s/\omega$, which is 0.282 nm in the case of the 22 THz peak observed in NaCl shocked along the [100] direction. Variations in phase across the surface of the shock front determine, in part, the emission characteristics through a phase-matching condition.

defects can have an effect similar to roughness in the shock front by generating phase variations of the polarization current across the shock surface.

Since the precise atomic-scale details of the shape of shock fronts vary under the variety of achievable experimental conditions, we have considered several example cases to explore the range of possible emission characteristics. The first case is that of an experimentally achievable shock front shape reported by Moore *et al.*[25] with a root-mean-square variation of 0.7 nm over a 75 μm area of the shock front. This shock was produced using a laser-drive technique.

Fig. 8 shows the spatial dependence of the electric field magnitude at 22 THz computed for the 22 THz peak from the 4.2 K NaCl [100] planar molecular dynamics simulation. The shock front is located at the center and the polarization (normal to the shock front plane) is in the vertical axis of the plot. Radiation is emitted in most directions except directly up and down (the shock propagation direction) because of the orientation of the polarization current direction. The emission appears approximately dipole-like in nature.

For a more planar shock front with less curvature, the radiation can be directed as in Fig. 9. This shock front shape is flatter than in Fig. 8 and includes a net tilt with respect to the crystal axis. The tilt angle is approximately 10^{-5} radians, which is achievable using laser-driven shocks by tilting the drive beam incidence angle. The tilt gives rise to a phase variation of the polarization current across the shock front that results in directed emission in a direction other than the shock propagation direction.

In the limiting case of a perfectly flat shock front with some tilt, the shock emits a directed collimated beam. The electric field magnitude in the beam is on the order of 0.1 V/cm for the 22 THz peak on the

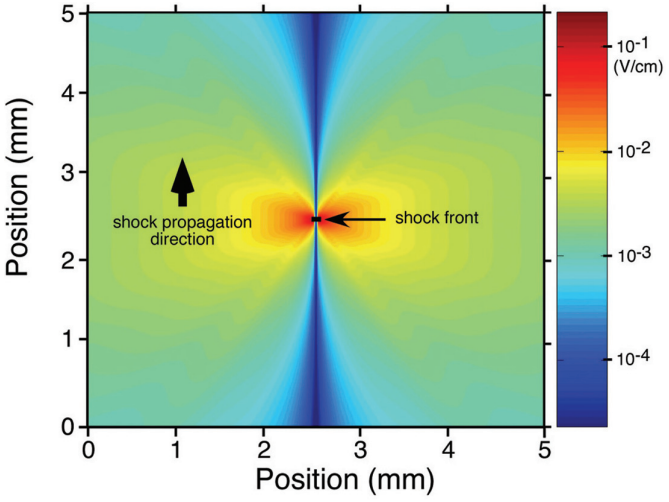

Fig. 8 Electric field magnitude at 22 THz from a 100 μm × 100 μm shock front for the 22 THz peak on the right side of Fig. 4 with a curved shock front based on an experimentally observed shock front[25].

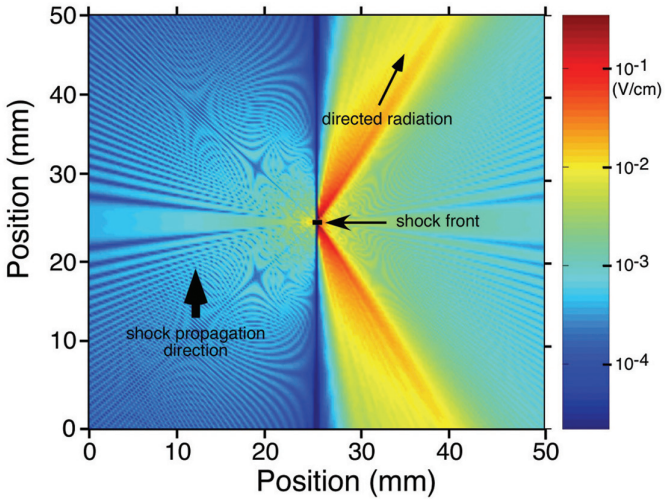

Fig. 9 Electric field magnitude at 22 THz from a 1 mm² shock front for the 22 THz peak on the right side of Fig. 4 with a curved, tilted shock front. Emission of directed radiation can be achieved for this sufficiently planar shock wave shape.

right side of Fig. 4. The collimated beam can be focused to enhance the electric field amplitude as is often done with terahertz sources. Field amplitudes may be increased by increasing the shock pressure (up to the point of irreversible material failure) and potentially through the use of other types of crystals.

Maxwell equation simulations

In addition to molecular dynamics simulations, we have performed direct numerical simulations of Maxwell's equations for a shock propagating through a model one-dimensional pyroelectric crystal[9]. While the model of the shocked crystal is simpler than the molecular dynamics simulations, the polarization, electric, and magnetic fields are all computed simultaneously within the simulation. Fig. 10 shows that nonzero frequency radiation is produced when the polarization is changed by the shock. As the shock propagates, it changes the value of the equilibrium static polarization. The resulting polarization current generates a spectrum of nonresonant polarization frequencies from zero to above 15 THz, shown in the bottom panel. The shock front, located around x = 120 nm, emits radiation to the left and right as it propagates to the right. The emitted radiation is narrowband despite the broad range of frequencies being excited. This is because the shock induces a coherent excitation of the polarization that only adds constructively at discrete frequencies, i.e. the sum over all polarizable elements has discrete frequency components but each individual polarizable element exhibits a broad range of frequency components. Using this model, we have shown that the magnitude of the emission

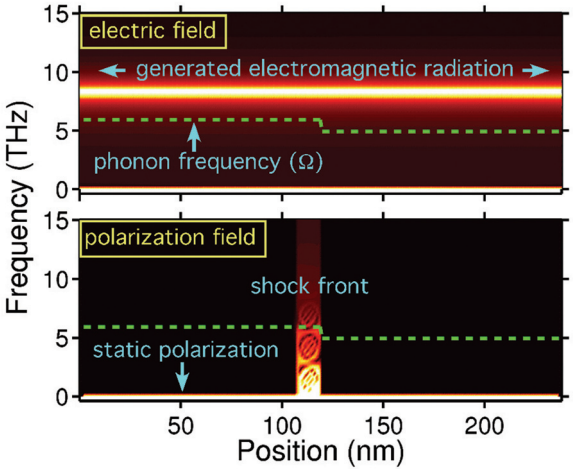

Fig. 10 Magnitude of the electric field (top) and polarization field (bottom) for a simulation of coherent radiation generation in a model of a shocked polarizable crystal. The shock propagates to the right and induces coherent oscillations in the polarization at the shock front (bottom). The polarization oscillations emit coherent radiation to the right and left (top). The shock front is located around x = 120 nm and the transverse optical phonon frequency (Ω) is depicted by the green dashed lines.

falls off rapidly when the shock front becomes spread out over many lattice planes of the crystal.

Discussion and conclusion

Shock-based terahertz radiation sources are likely to be rather inefficient since a considerable amount of energy is required to compress the material in addition to producing the radiation. While ultrafast lasers are not necessary to observe these effects, they are convenient for generating waves with initially fast rise times and also for common time-gated detection techniques. Ultrafast lasers are already used for an array of nonlinear terahertz sources and detectors.

Experimental observation of the coherent effect is anticipated to contain several challenges. Shock waves of a sufficient degree of planarity are most easily generated by laser-drive techniques[16], although it may also be possible to use gun-driven projectile approaches[26]. Crystal defects can result in diminished emission amplitudes, but large industries revolve around the growth of thin films of high-purity single crystals. Point defects are less likely to be problematic than line or other higher dimensional defects because they are less disruptive of the long-range crystalline order. Thin films of artificial crystals or nanostructures like GaN/AlN heterostructures can be grown with precisely designed, nanometer length scale lattice constants. Such structures are commonly grown for electronic devices and could be tailored to emit at a desired wavelength down to 1 THz and possibly below. One of the biggest challenges is likely to be detecting the relatively weak signals with existing technology. Detectors in this frequency regime are inefficient compared with optical techniques, but are developing rapidly[1]. As discussed in the section on radiation emission characteristics, the signal amplitude can vary widely depending on the details of the experiment. Such amplitudes may be detectable at frequencies above 10 THz using current nonlinear optical techniques that are often employed for terahertz detection. Much more sensitive terahertz photon counting techniques are being developed[27].

Other examples of techniques of radiation generation exist that are based on the general principle of a nonlinear excitation propagating through a periodic medium. One involves sending an ultrafast optical pulse through a periodically poled $LiNbO_3$ nonlinear optical crystal to generate terahertz radiation[28]. Another related technique is the generation of electromagnetic shock waves in periodic nonlinear transmission lines to generate radio-frequency radiation[29-31].

We have reviewed a new mechanism through which terahertz and infrared radiation can be generated: nonlinear strain (shock) waves in polarizable materials. High-frequency components can be spontaneously generated in such waves that couple to electromagnetic radiation through a variety of mechanisms, including ultrafast symmetry breaking and phase transformations. While generally weak and relatively inefficient, such sources may have novel properties, such as extremely long temporal coherence, that may be useful for some applications. The success of our initial experiments to observe terahertz radiation from a shocked material for the first time indicates that such sources may not be far from practical reality. We believe that the earliest and most immediate applications will be as diagnostics for ultrafast strain and shock waves. mt

Acknowledgments

We thank E. Ippen, F. Kaertner, K. Nelson of Massachusetts Institute of Technology; A. Taylor, R. Averitt, D. Moore, D. Funk, and S. McGrane of Los Alamos National Laboratory (LANL); L. Fried, D. Hicks, B. Sadigh and N. Holmes of Lawrence Livermore National Laboratory (LLNL); and W. Nellis of Harvard University for helpful discussions. This work was supported in part by the Materials Research Science and Engineering Center program of the National Science Foundation under Grant No. DMR-9400334. We acknowledge funding from the LLNL and LANL LDRD programs and the CINT user program. This work was performed in part under the auspices of the US Department of Energy by University of California, LLNL under Contract W-7405-Eng-48.

REFERENCES

1. Siegel, P. H., *IEEE Trans. Microwave Theory Technol.* (2002) **50**, 910
2. Siegel, P. H., and Dengler, R. J., *Proc. SPIE* (2004) **5354**, 1
3. Kemp, M. C., *et al.*, *Proc. SPIE* (2003) **5070**, 44
4. Chen, H.-T., *et al.*, *Nature* (2006) **444**, 597
5. Ferguson, B., and Zhang, X.-C., *Nat. Mater.* (2002) **1**, 26
6. Schmuttenmaer, C. A., *Chem. Rev.* (2004) **104**, 1759
7. Mueller, E. R., *The Industrial Physicist* (2003) **9** (4), 2
8. Reed, E. J., *et al.*, *Phys. Rev. Lett.* (2006) **96**, 013904
9. Reed, E. J., *et al.*, *Phys. Rev. E* (2007), in press
10. Reed, E. J., *et al.*, unpublished data
11. Sessler, A. M., and Vaughan, D., *Am. Sci.* (1987) **75**, 34
12. Koehl, R. M., and Nelson, K. A., *J. Chem. Phys.* (2001) **114**, 1443
13. Köhler, R., *et al.*, *Nature* (2002) **417**, 156
14. Williams, G. P., *Rev. Sci. Instrum.* (2002) **73**, 1461
15. Muskens, O. L., *et al.*, *Phys. Rev. Lett.* (2004) **92**, 035503
16. Gahagan, K. T., *et al.*, *Phys. Rev. Lett.* (2000) **85**, 3205
17. Patterson, J. E., *et al.*, *Phys. Rev. Lett.* (2005) **94**, 015501
18. Shkuratov, S. I., *et al.*, *Rev. Sci. Instrum.* (2004) **75**, 2766
19. Hauver, G. E., *J. Appl. Phys.* (1965) **36**, 2113
20. Linde, R. K., *et al.*, *J. Appl. Phys.* (1966) **37**, 2527
21. Harris, P., and Presles, H.-N., *J. Chem. Phys.* (1982) **77**, 5157
22. Strachan, A., *et al.*, *Phys. Rev. Lett.* (2003) **91**, 098301
23. Bringa, E. M., *et al.*, *J. Appl. Phys.* (2004) **96**, 3793
24. Zaretsky, E., *J. Appl. Phys.* (2003) **93**, 2496
25. Moore, D. S., *et al.*, *Appl. Phys. Lett.* (2001) **78**, 40
26. Holmes, N. C., *Rev. Sci. Instrum.* (1993) **64**, 357
27. Komiyama, S., *et al.*, *Nature* (2000) **403**, 405
28. Lee, Y.-S., *et al.*, *Appl. Phys. Lett.* (2000) **76**, 2505
29. Belyantsev A. M., and Klimin, S. L., *Izv. Vyssh. Uchebn. Zaved. Radiofiz.* (1993) **36**, 1011
30. Belyantsev, A. M. *et al.*, *Technical Phys.* (1995) **40**, 820
31. Seddon N. and Bearpark, T., *Science* (2003) **302**, 1537